

SPECTROSCOPIC STUDY OF CARBON MONOXIDE AND SODIUM COADSORPTION ON Ni(100)

F. ZAERA

Department of Chemistry, University of California, Riverside, CA 92521, U.S.A.

Submitted July 1988; accepted 29 August 1988

The coadsorption of carbon monoxide and sodium on Ni(100) single crystal surfaces has been studied by using TPD, XPS and HREELS. Sodium binds to nickel forming a monolayer that desorbs through a complex process, most probably involving cluster formation. Further exposure to sodium results in the condensation of Na multilayers that desorb with an activation energy of 17.5 kcal/mole. CO coadsorption with submonolayer coverages of sodium displays quite complicated TPD and HREELS spectra. It is clear, however, that there are at least two kinds of interactions between CO and Na. A short range interaction is manifested by higher CO binding energies, lower C-O stretching frequencies, and perhaps even direct Na-O interaction. We propose a tilted bonding configuration in this case. There is also longer range effects as seen at low sodium coverages by more subtle changes in desorption activation energies and in vibrational frequencies.

1. Introduction

The effect of alkali doping on transition metal catalyst is of great industrial importance. From a practical standpoint, alkali metals are additives for reactions such as methanation, Fischer-Tropsch and ammonia synthesis. Additionally, these systems have become quite popular in the scientific community because they represent a family of relatively simple systems where very rich and complex physical phenomena occur, including electron transferring and geometrical site blocking.

Extensive work has been published in the literature concerning the coadsorption of carbon monoxide and alkali metals on transition metal surfaces. Spectroscopic characterization of such systems using modern surface science techniques include reports for K on Fe(110), Fe(111), Fe(100) and Fe polycrystalline foils [1–4], K on Pt(111) and Pt(755) [5–7], K on Rh(111) [8], and Na, K and Cs on nickel surfaces [9–14]. In the present report we present results obtained for the coadsorption of CO and Na on Ni(100) by using thermal programmed desorption (TPD), X-ray photoelectron spectroscopy (XPS) and high-resolution electron energy loss spectroscopy (HREELS).

2. Experimental

The experiments were performed in a stainless steel ultra-high vacuum (UHV) chamber with a base pressure of 2×10^{-10} torr. The HREELS spectrometer consists of two fixed 127° cylindrical electrostatic deflectors arranged in a double "C" configuration, one acting as a monochromator for the incident beam and the other as an energy analyzer. An incident beam energy of 5 eV was used, with an energy resolution of 7–9 meV full-width-half-maximum (FWHM), as measured on the elastic peak. All spectra were recorded in the specular scattering direction with typical signals of $3\text{--}8 \times 10^5$ cps for the elastic peak and $1\text{--}3 \times 10^2$ cps for the loss features.

The quadrupole mass spectrometer was mounted so that the ionizer was enclosed in a gold plated cylinder with a coaxial entrance tube. The sample was positioned 1 mm from this tube for TPD experiments so that desorption only from the front face of the crystal would be detected. In addition, the gas dosers were terminated with capillary arrays in order to obtain high local pressures on the front face of the same, 20 to 50 times higher than the background pressure. A computer was utilized for the data acquisition during TPD in order to simultaneously monitor up to eight different masses.

A hemispherical energy analyzer was used for Auger electron (AES) and X-ray photoelectron (XPS) spectroscopies. An electron gun at a grazing incident angle to the crystal was the excitation source for AES while a double anode (Al-Mg) X-ray source was used for XPS. These techniques were employed in order to ensure the crystal cleanliness.

The Ni single crystal sample was cut along the (100) plane and polished using standard procedures. It was spot-welded to two tantalum wires attached to an L-shaped manipulator that provided 3 coordinates of displacement, full 360° rotation about the manipulator axis, and limited polar rotation of the surface plane. The sample could be resistively heated up to 1500 K, and cooled to 90 K using an internal liquid nitrogen reservoir located in the main axis of the manipulator. The crystal temperature was monitored using a chromel-alumel thermocouple spot-welded to the sample edge. A linear temperature programmer was used in the TPD experiments in order to achieve a constant 10 K/s heating rate over the complete temperature range.

Sodium was predosed using a Saes Getter source. Multilayer coverages were deposited by resistively heating the source for a few minutes. After extensive degassing metallic sodium could be deposited without adding significant amounts of carbon, oxygen or sulfur contamination, as checked by using AES and XPS. Submonolayer coverages were obtained by flashing the sample to a given temperature. The coverages measured by TPD and XPS as discussed below, and are reported as a fraction of saturation.

3. Results and discussion

We first studied the chemisorption of sodium on Ni(100). The thermal desorption behaviour after multilayer dosing at 90 K was studied by using mass spectrometry and X-ray photoelectron spectroscopy (fig. 1). Sodium desorption, followed by detecting the signal at 23 amu, displays two large peaks with maxima at 415 and 505 K respectively, and a small one around 650 K. The first peak displays an exponential front edge followed by an abrupt drop in signal after the maximum, characteristic of zero order kinetics. This peak is associated with the multilayer desorption, and a leading edge analysis yields a value of 17.5 ± 2.0 kcal/mole for the activation energy for desorption, quite a bit lower than the heat of sublimation for sodium as calculated using available thermodynamic data ($\Delta H_{\text{sub}}(300\text{--}400\text{ K}) = -26.0 \pm 0.3$ kcal/mole, ref. [15]).

The second peak corresponds to desorption from a monolayer of sodium. By assuming first order kinetics and using the peak width as well as its maximum [16] we obtain values of 20.0 ± 0.5 kcal/mole for the activation energy and 8.2 ± 0.3 for the logarithm of the preexponential factor. However, the peak shape is highly irregular and does not resemble those obtained for any simple desorption process. Assuming a more reasonable frequency factor of 10^{13} and using Redhead's equation we obtain an activation energy of 30 kcal/mole. We believe that more complex chemistry is taking place, perhaps the desorption of sodium

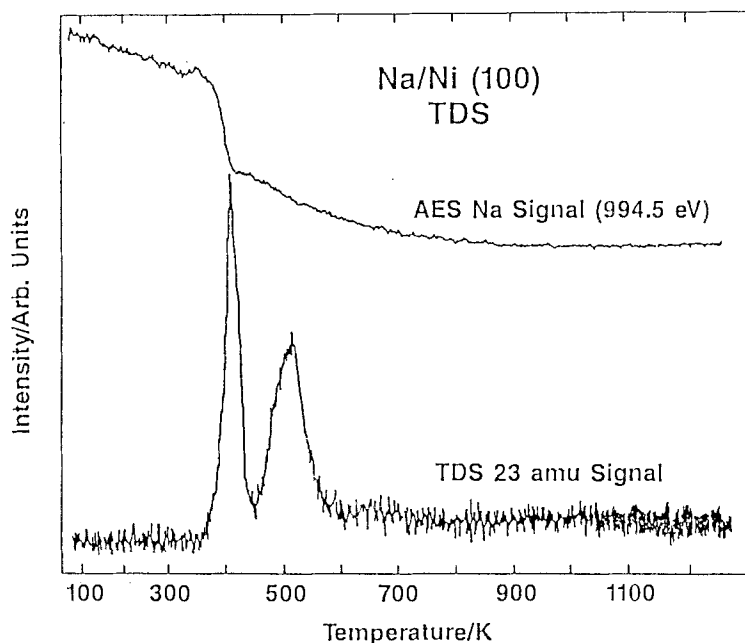


Fig. 1. Thermal desorption spectra of sodium adsorbed on Ni(100) surfaces. Shown are both the $\text{KL}_{23}\text{L}_{23}$ Na Auger and the 23 amu signals detected by an electron analyzer and a mass spectrometer respectively, as a function of crystal temperature. Heating rate = 10 K/s.

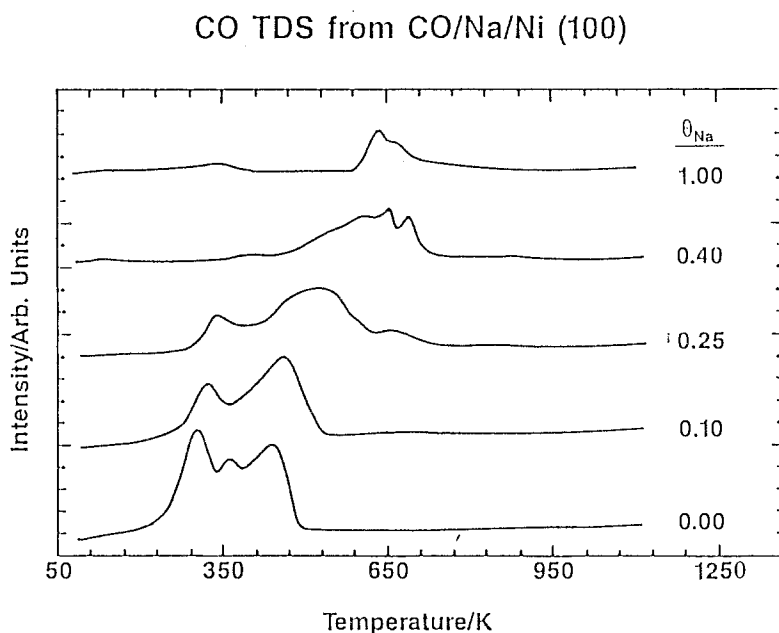


Fig. 2. CO thermal desorption spectra after CO saturation following several submonolayer dosings of sodium on Ni(100). Na coverages are given as a fraction of a monolayer. Heating rate = 10 K/s.

clusters. No peaks were detected at 46 amu, but this is not conclusive because the 23 amu is already quite weak and, if clusters were to form, they would fragment when ionized in the mass spectrometer. The TPD peak shape could also be explained by strong adsorbate-adsorbate interactions.

The desorption was also followed by recording the X-ray excited sodium $\text{KL}_{23}\text{L}_{23}$ Auger signal at 994.5 eV electron kinetic energy as a function of crystal temperature. The results, shown in fig. 1, are consistent with those obtained using the mass spectrometer, indicating that sodium is indeed desorbing and not diffusing into the bulk. The initial decrease in signal is due to an experimental artifact (the signal decrease because of the voltage drop across the sample, used in heating), but if this effect is eliminated, we could obtain a trace similar to the TPD spectrum by taking the derivative of the AES signal vs. temperature. The Auger signal was also used to determine the sodium coverage.

CO coadsorption on sodium predosed nickel surfaces was studied by TPD, XPS and HREELS. The thermal programmed desorption traces obtained for several sodium coverages and saturation of CO are shown in fig. 2. These spectra are quite complex, but a general trend can be easily seen where carbon monoxide bonds more strongly when sodium is present. Three overlapping peaks at 300, 365 and 447 are seen for CO desorption from a clean Ni(100) surface, in agreement with previously published spectra [17]. These peaks shift to higher temperatures for low coverages of sodium: peaks are detected at 320 and 470 K for $\theta_{\text{Na}} = 0.1$,

and at 340 and 475 K for $\theta_{\text{Na}} = 0.25$. For higher sodium coverages these peaks are replaced by new states at higher temperatures: maxima are seen at 520, 600 and 665 K for $\theta_{\text{Na}} = 0.25$; at 520, 605, 655 and 695 K for $\theta_{\text{Na}} = 0.4$; and at 635 and 680 K for $\theta_{\text{Na}} = 1.00$. Again, assuming first order desorption kinetics and 10^{13} s^{-1} preexponential factor, and using Redhead's equation, we see a shift in activation energies, from 19–28 kcal/mole at low sodium coverages, to close to 45 kcal/mole at saturation. Our coadsorption TPD results agree with those published by Kiskinova [10].

The area under the CO TPD traces has been used to estimate the carbon monoxide coverage at saturation as a function of sodium predose. The results are shown in fig. 3. It can be seen that, within our experimental error, sodium atoms block CO chemisorption sites in a linear fashion, that is, there is no indication of large ensemble sites required for either CO or Na adsorption. We did observe a small amount of empty sites available for CO chemisorption even at a monolayer coverage of sodium, but that could be justified by an error in sodium coverage

CO UPTAKE VS SODIUM COVERAGE

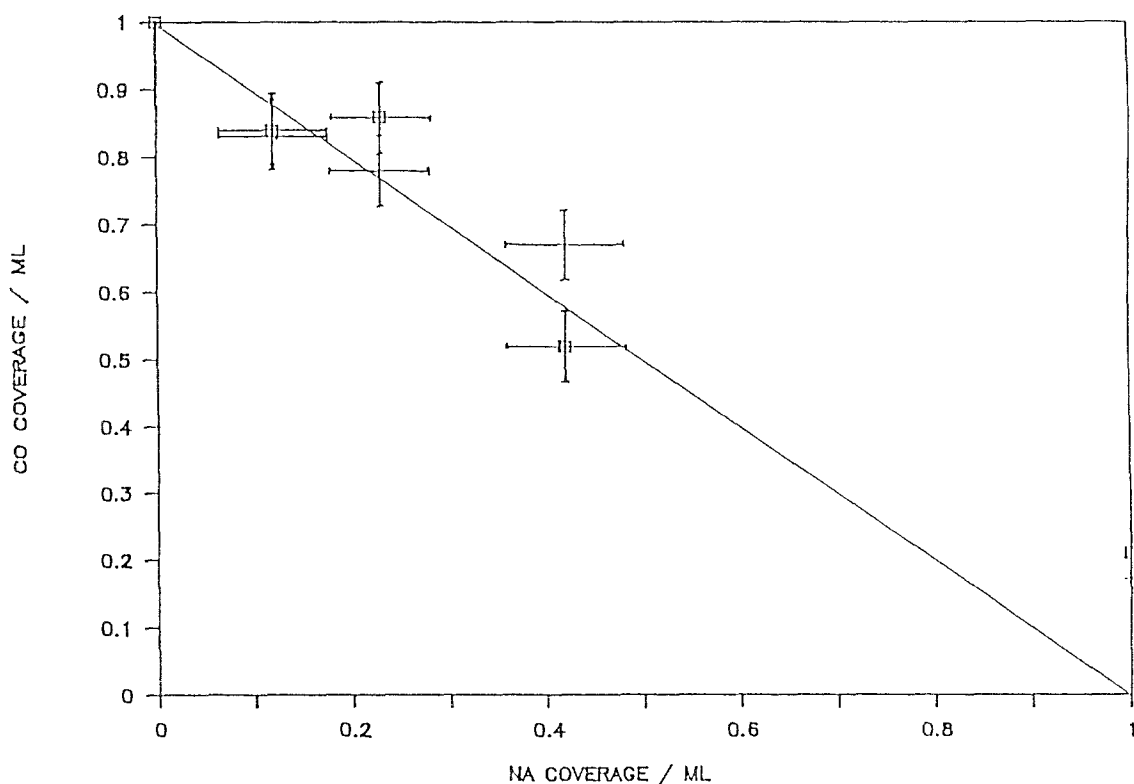


Fig. 3. CO coverage at saturation on sodium predosed Ni(100) surfaces as a function of sodium coverage. CO coverages were measured by the area under the TPD (□) and by following the C 1s XPS signal (+).

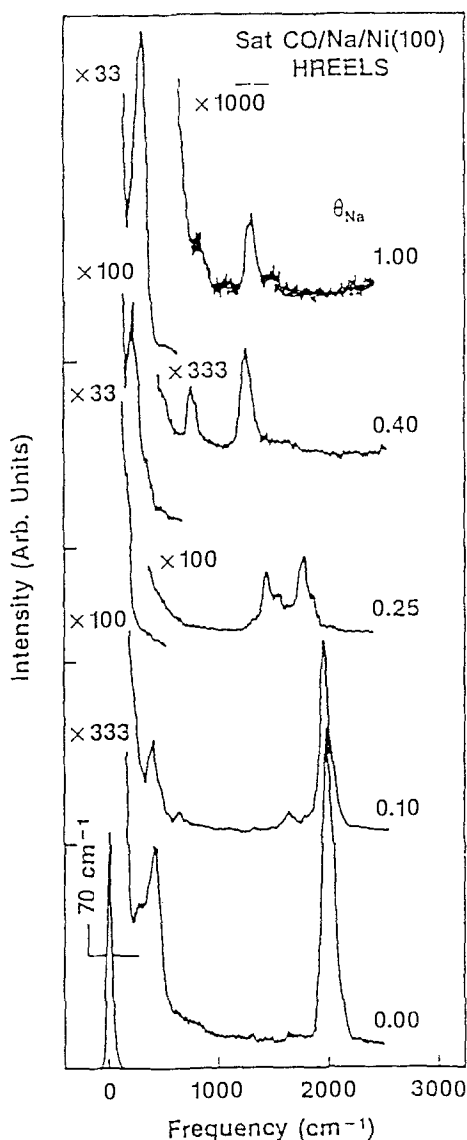


Fig. 4. HREELS spectra for CO coadsorbed with sodium on Ni(100) as a function of Na coverage. All spectra were taken at 90 K and correspond to saturation CO coverages.

determination or even by the existence of local defects in the packing of the sodium overlayer. Also shown in fig. 3 are the CO coverages as determined independently by the area under the C 1s XPS peak. As it can be seen, the XPS and TPD results are in good agreement.

Vibrational spectra, taken on the CO/Na/Ni system at several sodium initial coverages, are shown in fig. 4. The spectrum obtained for CO saturation on a clean Ni(100) surface contains two peaks at 420 and 1985 cm^{-1} , corresponding to

the Ni-CO and C-O stretching frequencies, respectively. This result indicates that all CO molecules sit on identical bridge sites, as reported previously [17]. The C-O stretch frequency shift to 1965 cm^{-1} at 10% Na coverage due to an increase in electronic density from backbonding from the nickel d to the CO π^* orbitals. This electron donation also strengthens the metal-carbon bond and is the reason for the increase in binding energy observed in the TPD. Additionally, there is another small peak at 1645 cm^{-1} . The intensity of this transition is about 10% of the main peak, and it could be assigned to CO molecules chemisorbed adjacent to the sodium atoms. Yates et al. have recently reported IR data on the CO/K/Ni(111) system that indicates the formation of “kernel” ensembles between CO and alkali atoms [18]. In this respect, the small peak at 645 cm^{-1} could be assigned to a Na-O stretch. Finally, the peak at 405 cm^{-1} corresponds to the Ni-CO stretch.

The vibrational spectra becomes quite complex at intermediate sodium coverages. For $\theta_{\text{Na}} = 0.25$ we can see at least four distinct peaks at 1440, 1555, 1765, and 1875 cm^{-1} . These could correspond to C-O stretching frequencies for CO chemisorbed on several sites and being affected to different levels by the presence of sodium. However, the almost disappearance of carbon-metal and/or oxygen metal stretching peaks also suggest the possibility of a change in bond geometry. Only shoulders at 130 and 260 cm^{-1} can be seen in the spectrum. The notion of tilted CO is not unreasonable, since that geometry has already been reported even on clean surfaces, namely, on Cr(110), Fe(100) and Mo(100) [19–21]. A chemisorption state with lower symmetry would have more dipole allowed vibrational transitions, and this could account for the several peaks observed in our HREELS results.

The high frequency peaks observed at 25% Na coverage disappear above $\theta_{\text{Na}} = 0.40$. At that coverage only peaks at 200, 755 and 1240 cm^{-1} can be seen. These values change to 280, 805 and 1280 cm^{-1} at even higher coverages ($\theta_{\text{Na}} = 1.00$). Again, the results would be justified by a model in which CO lies flat or tilted with respect to the surface. The dramatic reduction in frequency for the low energy peak, from 420 cm^{-1} to around 280 cm^{-1} could be explained by a new geometry where the carbon atom may be located on a hollow site, and so this band correspond to a collective vibration of the entire CO molecule with the surface. Alternatively, some of those peaks could be due to the interaction with sodium atoms. In any case, such low C-O stretch frequencies are not uncommon anymore, values as low as 1065 cm^{-1} have already been reported [22].

Alkali metals are commonly added to practical CO hydrogenation catalysts [23], although it is not clear if such additives increase the methanation activity. For the case of sodium on nickel, Huang and Richardson [24] report a maximum in methanation turnover frequency at 0.3 wt% sodium, but Kruissink et al. [25] only saw a monotonic poisoning with sodium coverage. Campbell and Goodman [26] studied the effect of potassium on Ni(100) and reported a steady decrease in methanation activity with K coverage, but an increase in CO dissociation rates.

The increase in carbon monoxide disproportionation with alkali coadsorption can be understood in view of our results. Addition of sodium to the nickel surface increases the CO binding energy and decreases the C-O bond strength. Our data even suggest that formation of a “tilted” CO, a configuration that could be viewed as the precursor for dissociation. The long range effect observed could account for the reported dramatic increase in C-O bond breaking at low alkali coverages [26]. However, in many of the conditions reported for the catalytic hydrogenation of CO, dissociation is not the limiting step, and poisoning of either H₂ adsorption or hydrogenation of carbon moieties have been proposed to be the reason for the decrease in methanation activity. Our results shed no light in this matter. Additionally, we did not detect any CO dissociation in our experiments. This process has a low probability on nickel even after dosing with alkali, and it can only be seen after high pressure CO exposures.

4. Conclusions

The coadsorption of carbon monoxide and sodium on Ni(100) single crystal surfaces has been studied by using TPD, XPS and HREELS. Sodium condenses at low temperatures, forming multilayer that desorb with an activation energy of 17.5 kcal/mole. A monolayer is held more strongly by the nickel surface, and its desorption kinetics is complex, suggesting the formation of sodium clusters.

CO coadsorption on nickel surfaces predosed with submonolayer quantities of Na display quite complex TPD with multiple and overlapping peaks. The HREELS at intermediate coverages is also complicated, but at low Na dosings two states can be identified, one for CO next to Na atoms and the second corresponding to the remaining CO. A strong short range interaction is clearly manifested at $\theta_{\text{Na}} = 0.1$ by a small peak at 1645 cm⁻¹ for the C-O stretching frequency. An additional weaker long range effect is seen for the remaining molecules, with a shift of 20 cm⁻¹ for the C-O stretch, and shifts of about 20 K in the TPD peaks, indicating a higher binding energy. The short range interaction is also seen at high sodium coverages, where vibrational stretch values as low as 1240 cm⁻¹ are seen, and activation energies for desorption are about 20 kcal/mole higher than on clean nickel. We also suggest that these CO molecules are bonded in a unique configuration, tilted with respect to the surface normal and perhaps with direct interaction between the oxygen and sodium atoms.

References

- [1] G. Brodén, G. Gafner and H.P. Bonzel, *Surf. Sci.* 84 (1979) 295.
- [2] J. Benziger and R.J. Madix, *Surf. Sci.* 94 (1980) 119.
- [3] J.B. Lee, M. Weiss and G. Ertl, *Surf. Sci.* 108 (1981) 357.

- [4] Z. Paál, G. Ertl and S.B. Lee, Appl. of Surf. Sci. 8 (1981) 231.
- [5] E.L. Garfunkel and G.A. Somorjai, Surf. Sci. 115 (1982) 441.
- [6] E.L. Garfunkel, J.E. Crowell and G.A. Somorjai, J. Phys. Chem. 86 (1982) 310.
- [7] M.P. Kiskinova, G. Pirug and H.P. Bonzel, Surf. Sci. 140 (1984) 1.
- [8] J.E. Crowell and G.A. Somorjai, Appl. Surf. Sci. 19 (1984) 73.
- [9] S. Andersson and U. Jostell, Surf. Sci. 46 (1974) 625.
- [10] M.P. Kiskinova, Surf. Sci. 111 (1981) 584.
- [11] H.S. Luftman, Y.-M. Sun and J.M. White, Appl. Surf. Sci. 19 (1984) 59.
- [12] H.S. Luftman, Y.-M. Sun and J.M. White, Surf. Sci. 141 (1984) 81.
- [13] K.J. Uram, L. Ng and J.T. Yates, Jr., Surf. Sci. 177 (1986) 253.
- [14] S. Bao, C.F. McConville and D.P. Woodruff, Surf. Sci. 187 (1987) 481.
- [15] C.R.C. *Handbook of Chemistry and Physics*, 55th ed. (CRC Press, Cleveland, 1974).
- [16] C.-M. Chan, R. Aris and W.H. Weinberg, Appl. Surf. Sci. 1 (1978) 360.
- [17] G.E. Mitchell, J.L. Gland and J.M. White, Surf. Sci. 131 (1983) 167.
- [18] K.J. Uram, L. Ng and J.T. Yates, Jr., Surf. Sci. 177 (1986) 253.
- [19] N.D. Shinn and T.E. Madey, Phys. Rev. Letters 53 (1985) 2481.
- [20] D.W. Moon, S. Cameron, F. Zaera, W. Eberhardt, R. Carr, S.L. Bernasek, J.L. Gland and D.J. Dwyer, Surf. Sci. 180 (1987) L123.
- [21] J.P. Fulmer, F. Zaera and W.T. Tysoe, J. Chem. Phys. 87 (1987) 7265.
- [22] F. Zaera, E. Kollin and J.L. Gland, Chem. Phys. Letters 121 (1985) 464.
- [23] P.H. Emmett, ed., *Catalysis*, Vol. 4 (Reinhold, New York, 1956) pp. 46–47, 330–334.
- [24] C.P. Huang and J.T. Richardson, J. Catal. 51 (1978) 1.
- [25] E.C. Kruissink, H.L. Pelt, J.R.H. Ross and L.L. Van Reijen, Appl. Catal. 1 (1981) 23.
- [26] C.T. Campbell and D.W. Goodman, Surf. Sci. 123 (1982) 413.